

Temperature sensor based on polymer thin film optical waveguide

Wang Longde^{1,2,3,4} Zhang Tong^{1,3,4} Zhang Xiaoyang^{1,3,4} Li Ruozhou^{1,3} Wang Luning¹

(¹School of Electronic Science and Engineering, Southeast University, Nanjing 210096, China)

(²Department of Chemistry and Chemical Engineering, Huainan Normal University, Huainan 232001, China)

(³Key Laboratory of Micro-Inertial Instrument and Advanced Navigation Technology of Ministry of Education, Nanjing 210096, China)

(⁴Suzhou Key Laboratory of Metal Nano-Optoelectronic Technology, Suzhou Research Institute of Southeast University, Suzhou 215123, China)

Abstract: Based on attenuated total reflection (ATR) and thermo-optic effect, the polymeric thin film planar optical waveguide is used as the temperature sensor, and the factors influencing the sensitivity of the temperature sensor are comprehensively analyzed. Combined with theoretical analysis and experimental investigation, the sensitivity of the temperature sensor is related to the thicknesses of the upper cladding layer, the waveguide layer, the optical loss of the polymer material and the guided wave modes. The results show that the slope value about reflectivity and temperature, which stands for the sensitivity of the polymer thin film temperature sensor, is associated with the waveguide film thickness and the guided wave modes, and the slope value is the highest in the zero reflectance of a certain transverse electric (TE) mode. To improve the sensitivity of the temperature sensor, the sensor's working incident light exterior angle α should be chosen under a certain TE mode with the reflectivity to be zero. This temperature sensor is characterized by high sensitivity and simple structure and it is easily fabricated.

Key words: temperature sensor; planar optical waveguide; guided wave mode; thermo-optic effect; prism coupling

doi: 10.3969/j.issn.1003-7985.2013.02.008

Optical sensors have a potential application for temperature measurement in areas such as scientific experiments, chemistry, biochemistry, and industrial process control. Temperature sensing based on optical techniques is promising and remains an area of continuing and intensive research interest in recent years^[1-3]. Fiber-

optic temperature sensors constitute a major category of the optical temperature sensors^[4-7]. Benefiting from the development of planar optical integration technology, optical sensors have been developed from using optical fiber as platforms to using easy-integrated planar waveguides. Currently, temperature sensors research based on optical planar waveguides is focused on surface plasmon resonance (SPR) sensors or other novel sensors^[8-12]. However, the studies in optical planar waveguide temperature sensors using prism coupling waveguides are relatively fewer. Especially, to the best of our knowledge, very few people use the high-order guided modes to measure temperature.

Polymers, owing to their high thermo-optic coefficients, have been considered for use in optical temperature sensors^[13-15]. In this paper we propose an optical sensor to measure temperature using the guided mode of a planar polymer optical waveguide. The principle of the sensor is based on the attenuated total reflection and the thermo-optic effects of polymer. Theoretical analysis and the experimental setup of the method are introduced and discussed in detail. We demonstrate the characteristics of the TE₀ mode and the higher-order TE modes in optical waveguide mode transmission using temperature sensing. The experiments demonstrate that the measurement range and ease of implementation are particular advantages of this technique.

1 Theoretical Analysis and Simulation

The proposed configuration of the sensor is shown in Fig. 1(a). The sensor consists of a high-index prism, an upper cladding layer, a SU8-2005 polymer thin film and a silica substrate. Under the substrate there is a heater plate. A transverse electric (TE) wave polarized laser beam is incident onto these films from the prism side.

When a TE-polarized light beam is incident on the base of the prism with an interior angle θ greater than the critical angle between the prism medium and the air layer, the incident light beam reflects at the interface of the prism and the air layer, and creates an evanescent field inside the air. At a synchronous incident interior angle θ , the evanescent field is phase-matched to the guided wave in

Received 2012-12-18.

Biographies: Wang Longde (1972—), male, graduate; Zhang Tong (corresponding author), male, doctor, professor, tzhang@seu.edu.cn.

Foundation items: The National Natural Science Foundation of China (No. 60977038), the Specialized Research Fund for the Doctoral Program of Higher Education (No. 20110092110016), the National Basic Research Program of China (973 Program) (No. 2011CB302004), the Foundation of Key Laboratory of Micro-Inertial Instrument and Advanced Navigation Technology of Ministry of Education of China (No. 201204).

Citation: Wang Longde, Zhang Tong, Zhang Xiaoyang, et al. Temperature sensor based on polymer thin film optical waveguide[J]. Journal of Southeast University (English Edition), 2013, 29(2): 152 – 157. [doi: 10.3969/j.issn.1003-7985.2013.02.008]

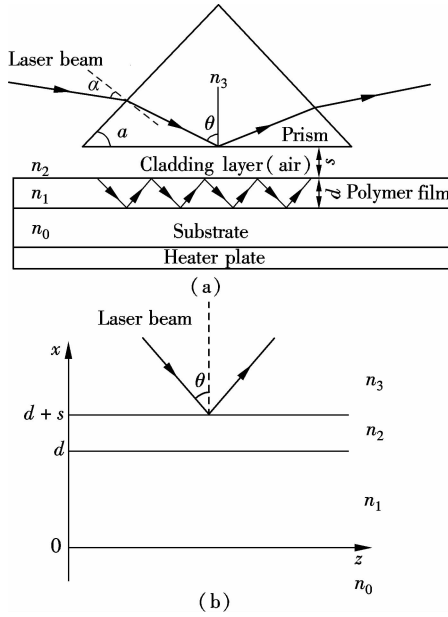


Fig. 1 Schematic diagram. (a) Proposed waveguide temperature sensor; (b) Representation of four-layer system

the polymer layer; that is to say, the interior angle θ of the incident light at wavelength λ satisfies the optical waveguide mode transmission condition, and the energy of incident light can be effectively coupled into the three-layer (air-polymer-fused silica) thin-film waveguide to excite guided waves, and the corresponding ATR resonance dips are shown on the reflection spectrum^[16]. Disregarding the prism face and the refraction of the input beam, the proposed sensor can be regarded as a four-layer system as shown in Fig. 1(b). For waveguide modes in this system to be excited, the following conditions must be satisfied: $n_2 < n_0 < n_1 < n_3$. n_0 , n_1 , n_2 and n_3 are the refractive indices of substrate, polymer, upper cladding layer and prism, respectively. According to the boundary condition of the electric field distribution, the reflectivity of the system can be written as^[17]

$$R = rr^* = |e^{i2\phi_{32}}|^2 \cdot \left[1 - \frac{4\text{Im}(\beta_0)\text{Im}(\Delta\beta)}{\{\beta - [\text{Re}(\beta_0) + \text{Re}(\Delta\beta)]\}^2 + [\text{Im}(\beta_0) + \text{Im}(\Delta\beta)]^2} \right] \quad (1)$$

where

$$\Delta\beta = \frac{-k_1 \sin 2\phi_{12} e^{-i2\phi_{12}} e^{-2p_2 s}}{2d_{\text{eff}}}, \quad d_{\text{eff}} = d + \frac{1}{p_0} + \frac{1}{p_2}$$

$$\phi_{12} = \arctan\left(\frac{p_2}{k_1}\right), \quad \phi_{32} = \arctan\left(\frac{p_2}{K_3}\right)$$

$$k_1 = (k_0^2 n_1^2 - \beta_0^2)^{1/2}, \quad k_3 = (k_0^2 n_3^2 - \beta_0^2)^{1/2}$$

$$p_0 = (\beta_0^2 - k_0^2 n_0^2)^{1/2}, \quad p_2 = (\beta_0^2 - k_0^2 n_2^2)^{1/2}$$

β_0 is the eigen propagation constant of the ideal three-layer waveguide in the absence of the prism; $\beta = k_0 n_3 \sin\theta$ is the propagation constant; k_0 is the wave vector in vacuum. When we consider the three-layer waveguide losses, we deduce the formula of β_0 , $\Delta\beta_1$, $\Delta\beta_2$ and $\Delta\beta_3$ as fol-

lows:

$$\beta_0 = \beta_{r0} + i(\Delta\beta_1 + \Delta\beta_2 + \Delta\beta_3)$$

$$\Delta\beta_1 = \frac{n_{1i} k_0^2 n_{1r}}{\beta_{r0} d_{\text{eff}}^0} \left(d + \frac{p_2}{k_1^2 + p_2^2} + \frac{p_0}{k_1^2 + p_0^2} \right)$$

$$\Delta\beta_2 = \frac{n_{2i} k_0^2 k_1^2 n_{2r}}{\beta_{r0} d_{\text{eff}}^0 p_2 (k_1^2 + p_2^2)}$$

$$\Delta\beta_3 = \frac{n_{0i} k_0^2 k_1^2 n_{or}}{\beta_{r0} d_{\text{eff}}^0 p_0 (k_1^2 + p_0^2)}$$

$$d_{\text{eff}}^0 = \left(d + \frac{1}{p_0} + \frac{1}{p_2} \right) \Big|_{\beta_{r0}}$$

where $\Delta\beta_1$, $\Delta\beta_2$, $\Delta\beta_3$ are considered as the change of β_0 with considering imaginary parts of n_1 , n_2 , n_0 ; β_{r0} is the eigen propagation constant of the ideal three-layer waveguide when n_1 , n_2 and n_0 are real numbers.

The imaginary parts of β_0 and $\Delta\beta$ are the intrinsic and radiative losses, respectively. The former represents the eigen loss in the ideal three-layer polymer waveguide, and the latter represents the leakage loss of the guided modes back into the prism. From Eq. (1), we can conclude that if $\text{Im}(\beta_0) = \text{Im}(\Delta\beta)$, then $R = 0$. That is to say, when the intrinsic loss is equal to the radiative loss, the minimal reflection R_{\min} of the ATR guided wave resonance dip is zero^[17].

Heating the polymer can change the propagation constant of the guided wave mode through the varying refractive index of the polymer due to the thermo-optic effect; thus, the synchronous incident exterior angle α and the minimal reflection R_{\min} of the ATR guided wave resonance dip are varied. The effective refractive index of each mode N_m is given by

$$N_m = n_3 \sin\theta = (n_3^2 - \sin^2\alpha)^{1/2} \sin\alpha - \sin\alpha \cos\alpha \quad (2)$$

From Eq. (2), we can obtain that

$$\alpha = \arcsin(\sin\alpha \sqrt{n_3^2 - N_m^2} - N_m \cos\alpha) \quad (3)$$

The mode indices for integral values of N are given by^[18]

$$N_m^2 = n_1^2 - \left(\frac{N\lambda}{2d_{\text{eff}}} \right)^2 \quad (4)$$

Substituting Eq. (4) into Eq. (3), we obtain

$$\alpha = \arcsin \left(\sin\alpha \sqrt{n_3^2 - n_1^2 + \left(\frac{N\lambda}{2d_{\text{eff}}} \right)^2} - \cos\alpha \sqrt{n_1^2 - \left(\frac{N\lambda}{2d_{\text{eff}}} \right)^2} \right) \quad (5)$$

where N is the number of modes, and $N = 1, 2, \dots$; λ is the laser wavelength; and d_{eff} is the effective thickness of the waveguide. The refractive index of the polymer layer is determined by plotting N_m^2 vs. N^2 . The polymer waveguide layer index and d_{eff} are then found by making a straight line extrapolation of the first two modes to $N = 0$ when such plots are made of the experimental data.

Through measuring the thermo-optic coefficient dn/dT

of the SU8 polymer by the SPA-4000 prism coupler containing a miniature heating device with an accuracy of $\pm 0.1^\circ\text{C}$ under the samples, we can obtain the relationships about the refractive index of polymer and temperature: $n_1 = 1.573\,07 - 1.34 \times 10^{-4}T$, $d = 1.33\,\mu\text{m}$; $n_1 = 1.572\,39 - 1.34 \times 10^{-4}T$, $d = 2.84\,\mu\text{m}$; $n_1 = 1.573\,45 - 1.38 \times 10^{-4}T$, $d = 4.09\,\mu\text{m}$; $n_1 = 1.572\,57 - 1.34 \times 10^{-4}T$, $d = 5.72\,\mu\text{m}$.

Substituting n_1 into Eq. (5), we can obtain the function of the light incident exterior angle α and the measurement temperature T .

The performance of a temperature sensor is associated with both the minimal reflection and the full width at half maximum (FWHM) of ATR resonance dip. The deep and narrow resonance dip allows a greater degree of modulation for a given temperature. The theoretical simulation results of Fig. 2 are the working base of the sensor under the conditions of $d = 4.09\,\mu\text{m}$, $n_1 = 1.568\,6 + 0.000\,3i$, $n_2 = 1.000 + 0.000\,01i$, $n_0 = 1.444\,2 + 0.000\,01i$, $n_3 = 1.934\,9$, $\lambda = 1\,550\,\text{nm}$, $T = 35^\circ\text{C}$. The guided modes are determined by changing the thickness of the coupling layer. It is known that the minimal reflection and FWHM of ATR resonance dip increase with the increase in the optical losses of the coupling layer and the guiding layer^[17, 19]. Once the materials of the coupling layer and the polymer are selected, the match condition illustrated by Eq. (1) can be reached by adjusting the thickness of the coupling layer and the guiding layer to make the intrinsic loss equal the radiative loss so that the minimal reflection of the resonance dip approaches zero.

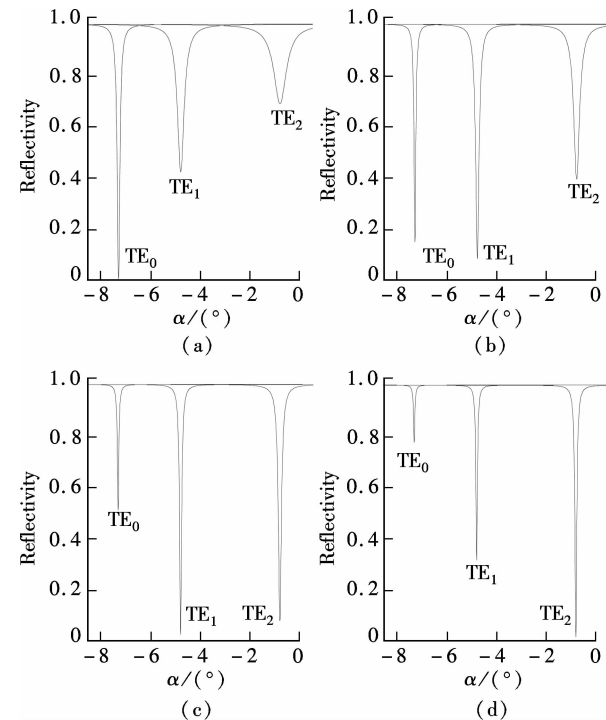


Fig. 2 Theoretical simulation resonance reflectivity dips TE modes for several thicknesses of the coupling layer. (a) $s = 150\,\text{nm}$; (b) $s = 250\,\text{nm}$; (c) $s = 350\,\text{nm}$; (d) $s = 450\,\text{nm}$

Because the imaginary part of β_0 changes with the thickness of the guiding layer, the minimal reflection of the resonance dip changes not only with the thickness of the coupling layer but also with the guiding layer. The properties of ATR resonance dip using the gas coupling layer can be optimized by choosing proper thicknesses of both the coupling layer and the guiding layer.

Figs. 3 and 4 are the theoretical plots from Eq. (1) of the minimal reflection of the resonance dip TE_0 vs. the thickness of the coupling layer and the guiding layer respectively. It can be seen that the thickness of the coupling layer and the guiding layer both contribute to the minimal reflection. Fig. 3 also shows that the FWHM of ATR resonance dip is relevant to the thickness of the coupling layer. The dips in the reflection intensity are due to the coupling of energy into the waveguide. The minimum position corresponds to the synchronous angle of the excitation mode and determines the working angle. The minimum value gives the maximum energy coupling efficiency and determines the sensitivity of the polymer thin film temperature sensor. The width of the dip is a function of the loss and determines the sensitivity of the temperature sensor. The modes are broadened due to attenuation by leakage both into the silica substrate and the prism. When

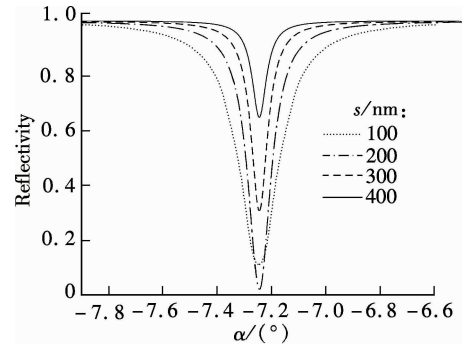


Fig. 3 Theoretical simulation resonance reflectivity dips TE_0 for several thicknesses of the coupling layer ($d = 4.0\,\mu\text{m}$, $n_1 = 1.576\,9 + 0.000\,3i$, $n_2 = 1.000 + 0.000\,01i$, $n_0 = 1.444\,2 + 0.000\,01i$, $n_3 = 1.934\,9$, $\lambda = 1\,550\,\text{nm}$, $T = 30^\circ\text{C}$)

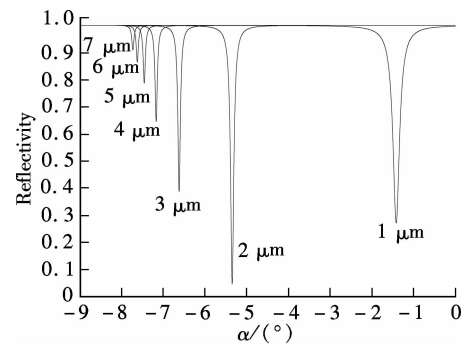


Fig. 4 Theoretical simulation resonance reflectivity dips TE_0 for several thicknesses of the guiding layer ($s = 400\,\text{nm}$, $n_1 = 1.576\,9 + 0.000\,3i$, $n_2 = 1.000 + 0.000\,01i$, $n_0 = 1.444\,2 + 0.000\,01i$, $n_3 = 1.934\,9$, $\lambda = 1\,550\,\text{nm}$)

the thickness of the coupling layer $s = 400$ nm, the width of the resonance dip is narrow. From Fig. 5, we know that the reflectivity is a function of the angle of incidence and the thickness of the guiding layer. The sensor's working incident exterior angle can be chosen to be TE_0 in lower thicknesses or higher-order TE modes in higher thicknesses of the waveguide.

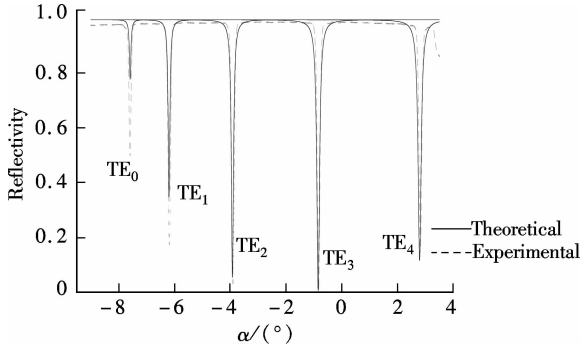


Fig. 5 Theoretical and experimental ATR spectra of the thickness of 5.72 μm guiding layer waveguide

2 Experimental Results and Discussion

In our experiment the refractive index of the prism is $n_3 = 1.9654$ at the wavelength of 1550 nm. Selecting the SU8-2005 polymer as the optical waveguide material is due to the fact that the SU8 has a higher thermo-optic coefficient and a lower propagation loss and it also has the ability of forming stable films. The polymer thin-films of 1.33, 2.84, 4.09 and 5.72 μm are spin-coated onto the polished fused Silica substrate, pre-baked at 95 $^{\circ}\text{C}$ for 120 s, then cured by UV-exposure for 2 s and finally baked at 95 $^{\circ}\text{C}$ for 12 h in an oven to complete removal of the solvent from the film. The SU8 polymer solution is then filtered through a 0.22 μm filter before it is applied.

The ATR spectra of the multilayer waveguide system are generated as shown in Fig. 5. Several resonance dips that correspond different guided modes are shown in the spectrum in choosing the sensor's working interior angle to be near the TE_3 resonance dip. The experimental result of light reflectivity for TE_0 vs. the temperature in different thicknesses of the guiding layer for the proposed waveguide sensor is shown in Fig. 6. From Fig. 6 we know that the reflectivity and temperature is in accord with a good linear relationship at 36 to 43 $^{\circ}\text{C}$. The results show that the slope which stands for the sensitivity of the polymer thin film temperature sensor is associated with the waveguide film thickness and the guided modes. Fig. 7 shows the theoretical results of the light reflectivity vs. the temperature in different thicknesses of the guiding layer for the waveguide temperature sensor. From Fig. 7 it can be obtained that the theoretical result is consistent with the experimental result in Fig. 6. The slope is relevant to TE modes but not relevant to the thickness of the guiding layer when the imaginary part of n_1 does not

change with the thickness of the guiding layer.

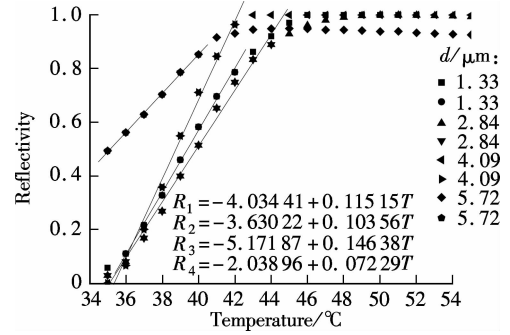


Fig. 6 Experimental results of light reflectivity vs. measurement temperature in different thicknesses of guiding layer for proposed waveguide sensor ($m = 0$)

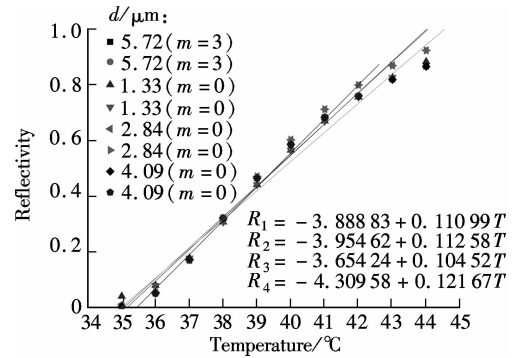


Fig. 7 Theoretical results of light reflectivity vs. measurement temperature in different thicknesses of the guiding layer for proposed waveguide sensor ($n_{1i} = 0.0003i$, $n_2 = 1.000 + 0.00001i$, $n_3 = 1.4442 + 0.00001i$, $\lambda = 1550$ nm)

Figs. 8 and 9 show the light reflectivity of TE_1 and TE_2 vs. the temperature in different thicknesses of the guiding layer for the proposed waveguide sensor. From Figs. 6, 8 and 9, we can obtain that for the same guiding layer thickness, the slope decrease with the increase in the guided modes when reflectivity is zero for TE_0 . For instance, if the thickness of the guiding layer is 4.09 μm , the slope values of TE_0 , TE_1 , TE_2 are 0.14638, 0.08385, 0.04688, respectively. Nevertheless, for a film thickness of 5720 nm, the slope values of TE_0 , TE_1 ,

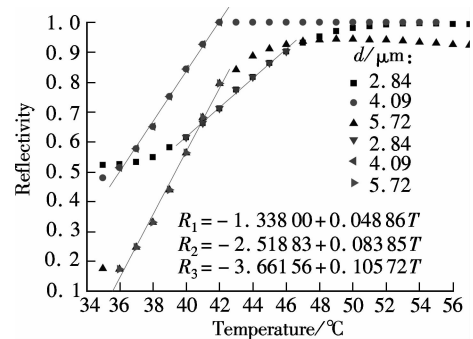


Fig. 8 Light reflectivity of TE_1 vs. measurement temperature in different thicknesses of the guiding layer for proposed waveguide sensor ($m = 1$)

TE₂ and TE₃ are 0.072 29, 0.105 72, 0.114 5, 0.121 67, respectively. The slope value is the highest in TE₃ where the reflectivity is zero in Fig. 5. Therefore, to improve the sensitivity, the sensor’s working incident light exterior angle α can be chosen to be in a certain TE mode in which the reflectivity is zero. Fig. 10 shows the theoretical and experimental light incident exterior angle α of TE vs. the temperature of the guiding layer for the waveguide sensor. The experimental results are in agreement with the results derived from Eq. (5) and experimental data n_1 .

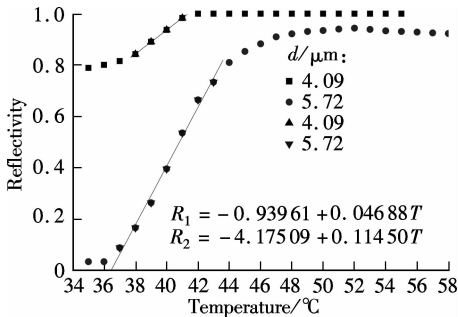


Fig. 9 Light reflectivity of TE₂ vs. measurement temperature in different thicknesses of the guiding layer for proposed waveguide sensor ($m = 2$)

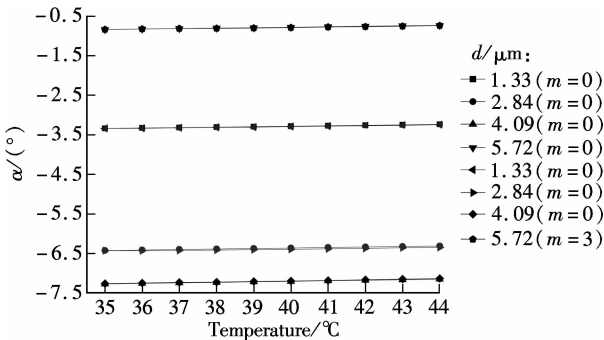


Fig. 10 Theoretical and experimental light incident exterior angle of TE vs. measurement temperature of the guiding layer for proposed waveguide sensor

3 Conclusion

We demonstrate a polymer thin film waveguide temperature sensor based on guided wave resonance with the ATR structure. The property of the polymer thin film optical waveguide temperature sensor is heavily dependent on the planar optical guiding modes, the loss of the polymer, the thickness of the guiding layer and the cladding layer. The relationships among temperature, refractive index, reflectivity, TE modes and the incident light exterior angle of the prism are systematically investigated. The slope about reflectivity and temperature which stands for the sensitivity of the polymer thin film temperature sensor is associated with the waveguide film thickness and the guided modes. The sensor’s working incident light exterior angle α should be chosen under a certain TE mode with

the reflectivity to be zero, and, in this case, the temperature sensor has the highest sensitivity. This temperature sensor is characterized by high sensitivity and simple structure and it is easily fabricated.

References

[1] Andersen T B, Han Z H, Bozhevolnyi S I. Compact on-chip temperature sensors based on dielectric-loaded plasmonic waveguide-ring resonators[J]. *Sensors*, 2011, **11** (2): 1992 – 2000.

[2] Childs P R N, Greenwood J R, Long C A. Review of temperature measurement[J]. *Rev Sci Instrum*, 2000, **71** (8): 2959 – 2978.

[3] Chen J H, Huang X G, He W X, et al. A parallel-multi-point fiber-optic temperature sensor based on Fresnel reflection[J]. *Optics and Laser Technology*, 2011, **43**(8): 1424 – 1427.

[4] Lee B. Review of the present status of optical fiber sensors[J]. *Opt Fiber Technol*, 2003, **9**(2): 57 – 79.

[5] Sharma A K, Jha R, Gupta B D. Fiber-optic sensors based on surface plasmon resonance: a comprehensive review[J]. *IEEE Sens J*, 2007, **7**(8): 1118 – 1129.

[6] Remouche M, Georges F, Meyrueis P. Flexible optical waveguide bent loss attenuation effects analysis and modeling application to an intrinsic optical fiber temperature sensor[J]. *Optics and Photonics Journal*, 2012, **2**(1): 1 – 7.

[7] Zeng X, Wu Y, Hou C L, et al. A temperature sensor based on optical microfiber knot resonator [J]. *Optics Communications*, 2009, **282**(18): 3817 – 3819.

[8] Lee S M, Ahn K C, Sirkis J S. Planar optical waveguide temperature sensor based on etched bragg gratings considering nonlinear thermo-optic effect[J]. *KSME International Journal*, 2001, **15**(3): 309 – 319.

[9] Lee D R, Cho K M, Jang S W, et al. Side-polished fiber optic temperature sensor using a prism and fiber-to-planar waveguide coupler[J]. *Microwave and Optical Technology Letters*, 2005, **46**(6): 523 – 525.

[10] Dumais P, Callender C L, Noad J P, et al. Temperature sensors and refractometers using liquid-core waveguide structures monolithically integrated in silica-on-silicon [C]//*Proceedings of SPIE on Optical Sensors and Detectors*. Montréal, Canada, 2008, **7099**: 1 – 11.

[11] Remouche M, Mokdad R, Chakari A, et al. Intrinsic integrated optical temperature sensor based on waveguide bend loss [J]. *Optics and Laser Technology*, 2007, **39** (7): 1454 – 1460.

[12] Seo J K, Kim K J, Oh M C. Integrated-optic temperature sensors based on guided-mode radiation in polymer waveguide[J]. *Optics Communications*, 2010, **283**(7): 1307 – 1310.

[13] Rindorf L, Bang O. Highly sensitive refractometer with a photonic-crystal-fiber long-period grating[J]. *Optics Letters*, 2008, **33**(6): 563 – 565.

[14] Jung W G, Kim S W, Kim K T, et al. High-sensitivity temperature sensor using a side-polished single-mode fiber covered with the polymer planar waveguide [J]. *IEEE Photonics Technology Letters*, 2001, **13** (11): 1209 – 1211.

[15] Chen J G, Zhang T, Zhu J S, et al. Low-loss planar optical waveguides fabricated from polycarbonate[J]. *Polymer Engineering and Science*, 2009, **49** (10): 2015 – 2019.

[16] Tien P K, Ulrich R. Theory of prism-film coupler and thin-film light guides[J]. *J Opt Soc Am*, 1970, **60**(10): 1325 – 1337.

[17] Deng X X, Cao Z Q, Shen Q S, et al. An improved configuration of reflective-type electro-optic modulator with high light-induced damage threshold[J]. *Optics Communications*, 2004, **242**(4): 623 – 630.

[18] Lee H J, Henry C H, Orlowsky K J, et al. Refractive-index dispersion of phosphosilicate glass, thermal oxide, and silicon nitride films on silicon[J]. *Applied Optics*, 1988, **27**(19): 4104 – 4109.

[19] Koynov K, Goutev N, Fitrilawati F, et al. Nonlinear prism coupling of waveguides of the conjugated polymer MEH-PPV and their figures of merit for all-optical switching[J]. *J Opt Soc Am B*, 2002, **19**(4): 895 – 901.

有机聚合物薄膜波导温度传感器

王龙德^{1,2,3,4} 张 彤^{1,3,4} 张晓阳^{1,3,4} 李若舟^{1,3} 汪鲁宁¹

(¹ 东南大学电子科学与工程学院,南京 210096)

(² 淮南师范学院化学与化工系,淮南 232001)

(³ 教育部微惯性仪器及先进导航技术重点实验室,南京 210096)

(⁴ 东南大学苏州研究院苏州市金属纳米光电技术重点实验室,苏州 215123)

摘要:基于棱镜耦合衰减全反射和波导材料热光效应,利用聚合物薄膜平板波导作为温度传感器,论证了影响温度传感器灵敏度的各种因素.结合理论分析及实验验证,温度传感器灵敏度不仅与平板波导上包层及芯层厚度、聚合物材料光学损耗有关,而且与波导的导波模式阶数有关.结果表明,反映温度传感器反射率与温度关系灵敏度的斜率在反射率为零的某阶 TE 模式下,其值最高.因此,为提高传感器的灵敏度,传感器的入射光外角应选择在反射率为零的某阶 TE 模式下工作.该聚合物薄膜波导温度传感器具有灵敏度高、结构简单及易制作等特点.

关键词:温度传感器;平板波导;导波模式;热光效应;棱镜耦合

中图分类号:O431.1